PERGAMON

International Journal of Multiphase Flow 27 (2001) 1579–1602

International Journal of Multiphase Flow

www.elsevier.com/locate/ijmulflow

Evolution of statistical parameters of gas–liquid slug flow along vertical pipes

R. van Hout *, D. Barnea, L. Shemer

Department of Fluid Mechanics and Heat Transfer, Faculty of Engineering, Tel-Aviv University, Tel-Aviv 69978, Israel

Received 10 August 2000; received in revised form 13 February 2001

Abstract

The evolution of hydrodynamic and statistical parameters along the pipe was studied experimentally in gas–liquid slug flow for various flow conditions and two pipe diameters. The measuring modules comprise a set of three adjacent optical fiber probes and could be easily transferred to various positions along the pipes. The probes detect the passage of the gas–liquid interface. This technique enables one to measure the instantaneous velocities of nose and tail of elongated (Taylor) bubbles simultaneously with the slug length ahead of each bubble. The liquid slug and Taylor bubble length distributions along the pipe, together with the dependence of the Taylor bubble velocity on the liquid slug length ahead of it, are presented at various locations along the pipe. Empirical correlations relating the Taylor bubble velocity with the bubble separation distance are suggested. These correlations are used as an input to a model for slug length distribution. The model results are compared with the experiments. © 2001 Elsevier Science Ltd. All rights reserved.

Keywords: Two-phase flow; Slug flow evolution; Slug length distribution; Interface propagation velocity

1. Introduction

Gas–liquid slug flow in pipes occurs over a broad range of gas and liquid flow rates. It is one of the most complex flow patterns that is characterized by intermittent and transient behavior. In vertical slug flow most of the gas is located in large bullet-shaped bubbles (Taylor bubbles) which span most of the pipe cross-section. The Taylor bubbles are separated by liquid slugs, which usually contain small dispersed bubbles. The liquid confined between the Taylor bubbles and the pipe wall flows around the bubble as a thin film. The unsteady nature of slug flow makes the prediction of pressure drop and heat and mass transfer a difficult task. Most models that deal with steady slug flow, assume constant lengths and shapes of liquid slugs and elongated bubbles, as

* Corresponding author.

PII: S0301-9322(01)00016-7

well as a constant Taylor bubble propagation velocity (Dukler and Hubbard, 1975; Fernandes et al., 1983; Taitel and Barnea, 1990). However, due to the intrinsically unsteady and irregular character of slug flow, statistical means are required for its proper description. The knowledge of the time-averaged values of the flow parameters is not always sufficient and information regarding the distributions of these parameters is often essential. Of particular importance is the maximum possible slug length since slug catchers design depends on the longest encountered slug and not necessarily on the average one. Moreover, transients are rather frequent and the development of the liquid slug and Taylor bubble length distributions from undeveloped to developed slug flow should be considered.

The evolution of Taylor bubble and liquid slug length distributions along the pipe can be understood as follows. Bubbles behind short slugs usually travel faster than those behind long slugs and will therefore overtake the leading bubbles. During the merging process, the liquid slug length as well as the Taylor bubble length increases. The process of overtaking is assumed to be terminated once the velocity profiles at the back of all the slugs are fully developed and all the bubbles propagate at the same translational velocity.

The translational velocity of a Taylor bubble U_{tr} has been studied extensively. It is assumed to be a superposition of the velocity of the bubble in stagnant liquid, i.e. the drift velocity U_d, and an additional contribution of the slug mixture velocity U_m (Nicklin et al., 1962):

$$U_{tr} = CU_m + U_d. \tag{1}$$

The value of the constant C is based upon the assumption that the bubble follows the maximum local velocity in front of the nose tip (Nicklin et al., 1962; Bendiksen, 1984; Shemer and Barnea, 1987; Polonsky et al., 1999b). Therefore C, which is the ratio U_{max}/U_m equals approximately 1.2 for fully developed turbulent flow and 2.0 for laminar flow.

However, the translational velocities of elongated bubbles are not constant in continuous slug flow, especially in the entrance region, and depend on the separation distance between two consecutive bubbles. At small separation distances, trailing bubbles accelerate and eventually merge with the leading Taylor bubble (Moissis and Griffith, 1962; Hasanein et al., 1996; Fagundes Netto et al., 1998; Pinto et al., 1998; Aladjem Talvy et al., 2000). The merging process continues until the liquid slugs are long enough, so that the velocities of the trailing bubbles are unaffected by the leading ones. Different models have been suggested to simulate the merging process and to calculate the minimum stable slug length. Moissis and Griffith (1962), Taitel et al. (1980) and Barnea and Brauner (1985) suggested that the developed slug length is equal to the distance at which the wall jet generated by the liquid film around the elongated bubble is absorbed by the liquid slug. This approach yields the minimum stable slug length $16D$ for vertical flow. A hydrogen bubble technique to visualize the instantaneous velocity profiles in slug flow was applied by Shemer and Barnea (1987). They suggested a minimum stable slug length of $20D$ for vertical flow. Aladjem Talvy et al. (2000) performed a controlled injection of bubbles into stagnant liquid to study the acceleration and coalescence of two consecutive bubbles using a flow visualization technique. It was found that even for large separation distances (up to $60D$, the upper limit of their measurement range), the trailing bubble generally travels faster than the leading one.

The merging process in the course of the slug flow evolution strongly affects the variation of both the slug length and the Taylor bubble length distributions along the pipe. Little work has been carried out to determine slug length distributions. Bernicot and Drouffe (1989) proposed a

probabilistic approach for slug formation at the entrance of a nearly horizontal pipe. The length distributions were modeled using deterministic equations. Barnea and Taitel (1993) developed a simplified model that computes the slug length distribution at any desired position along the pipe. The development of the liquid slug distribution along the pipe depends on the relative translational velocities of two consecutive Taylor bubbles. The model tracks each individual bubble as it propagates along the pipe. The translational velocity of a bubble as a function of the liquid slug length ahead of it has to be given as an input relation.

Experimental work concerning the liquid slug and Taylor bubble length distributions has been carried out mainly for horizontal or slightly inclined slug flow. The liquid slug length distribution in horizontal flow was found to be described well by positively skewed theoretical distributions as the log-normal, the gamma or the inverse Gaussian distributions (Brill et al., 1981; Dhulesia et al., 1991). The dependence of the liquid slug distribution in large pipe diameters ($D = 0.2$ and 0.4 m) on both the pipe diameter and the position along the pipe was investigated by Dhulesia et al. (1991). It was found that the slug length and its standard deviation increase with pipe diameter. The slug length distributions developed from peaked distributions (at 77 and 166 m from the inlet) to more dispersed distributions near the pipe outlet (333 m from inlet). Sæther et al. (1990) concluded that the slug length in horizontal pipe flow obeys fractal statistics. Therefore, in order to predict the slug length at a fixed point along the pipe, the Hurst exponent, the average slug length and the standard deviation have to be known. Cook and Behnia (2000) compared experimental liquid slug length distributions at 10 m from the inlet to distributions computed by the model of Barnea and Taitel for a 50 mm pipe. The experiments and model compared well. In vertical slug flow, van Hout et al. (1992) measured liquid slug and Taylor bubble length distributions in a 0.054 m diameter pipe. Recently, Costigan and Whalley (1997) performed similar measurements in a 0.032 m diameter pipe. In both cases the measurements were performed at about 6 m from the inlet section. Costigan and Whalley (1997) concluded that the bubble and slug lengths are approximately normally distributed. Hasanein et al. (1996) measured the liquid slug length distributions for air–kerosene mixture at 2 m from the inlet of a 0.0254 m pipe. The general shape and statistical parameters of the distributions compared well to the predictive model of Barnea and Taitel (1993).

The aim of the present work is to provide detailed information about the evolution of some hydrodynamic parameters of air–water slug flow in vertical pipes. Experiments were carried out for two different pipe diameters. The experimental results are compared to those obtained by the application of a predictive model.

2. Experimental facility and measurement method

A schematic layout of the experimental facility is shown in Fig. 1. The system consists of a steel frame supporting two parallel transparent 10 m long Perspex pipes with internal diameters of 0.024 and 0.054 m. The frame can be rotated around its axis from horizontal to vertical position. The present experiments were carried out for vertical upward flow. The pipes consist of sections about 2 m long, connected by easily loosened and fastened flanges.

Air was supplied from a central high-pressure line and passed through an oil filter and a pressure reducer. The pressure reducer maintained a constant gage pressure of 1 bar. The air flow

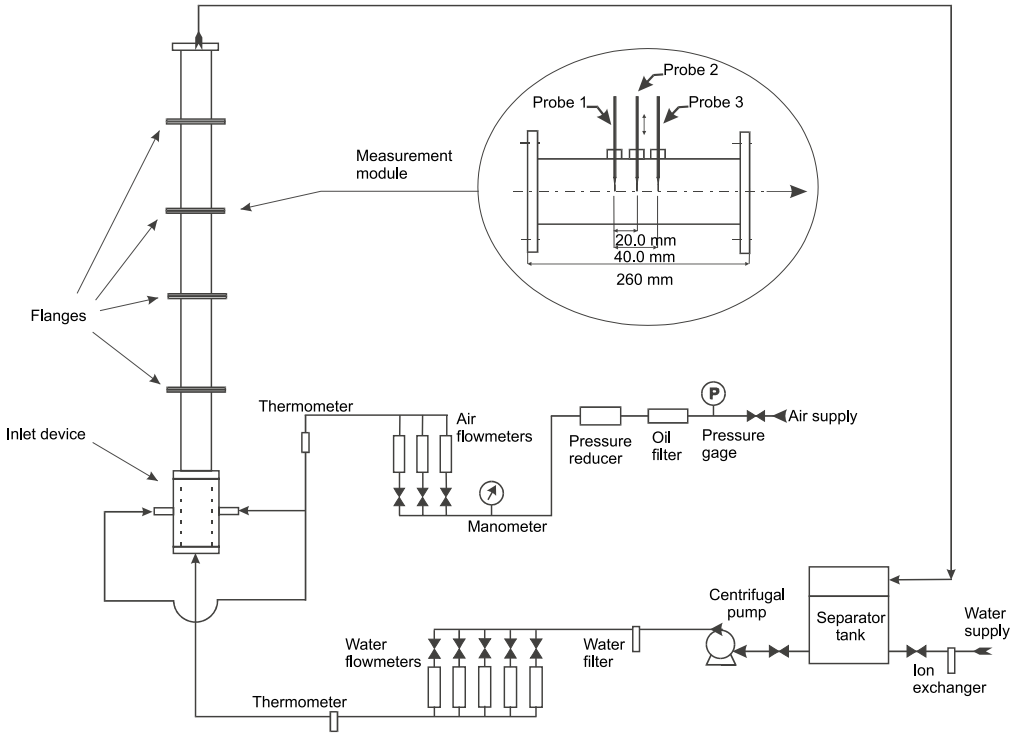

Fig. 1. Layout of the experimental system and the measuring module.

rate was measured by a system of three rotameters. A mercury manometer was incorporated to ensure a constant inlet pressure.

Tap water was first filtered by particle filters, deionized, and then circulated in a closed loop via a 1500 l separator tank through the system by a frequency-controlled centrifugal pump. In order to ensure clean water conditions, a 22 μm water filter was installed. The liquid flow rate was controlled by a system of five rotameters. The inlet temperatures of the two phases were measured by two thermometers located at the entrance of the test section.

The two fluids were introduced through a "mixer"-type 30 cm long inlet device. The device is an annulus with an inner pipe of the same diameter as that of the test section and a gap of 2.5 cm between the two pipes. The inner pipe was perforated with uniformly distributed 1 mm holes, 10 mm apart in the axial direction and 5 mm apart on the circumference in a staggered configuration. Water entered in the axial direction. Air was introduced into the gap of the annulus and entered the test section through the holes in the inner pipe.

Experiments in the slug flow regime were carried out in both pipes for the following pairs of water and gas superficial velocities: (a) $U_{LS} = 0.01$ m/s, $U_{GS} = 0.41$ m/s and (b) $U_{LS} = 0.1$ m/s, $U_{GS} = 0.63$ m/s. In the 0.054 m pipe, additional experiments were carried out for $U_{LS} = 0.25$ m/s, $U_{GS} = 0.41$ m/s. Note that the gas flow rates are given for the outlet pressure of 0.1 MPa.

Measurements were performed using optical fiber probes that are sensitive to the change in the refractive index of the surrounding medium and thus are capable of detecting the local instantaneous phase (gas or liquid). Commercially available optical fiber probes (Photonetics type FES)

Table 1
Position of the sampling stations along the pipe

Station	$D = 0.054$ m		$D = 0.024$ m	
	x (m)	x/D	x (m)	x/D
A	0.91	16.8	0.365	15.2
B	2.72	50.4	0.80	33.3
C	4.79	88.7	2.82	117.5
D	6.86	127.0	4.85	202.1
E			6.88	286.7

were used. The sensitive silica probe tip has a diameter of 0.14 mm. The return signals from the optical fiber sensors were amplified to yield an analog output of two levels representing the instantaneous phase of the medium present at the fiber tip. The analog output signals (0–10 V) were sampled by a 12-bit A/D converter with a maximum total sampling frequency of 100 kHz. More details on this technique can be found in van Hout et al. (1992).

Four optical probes were used simultaneously. One of the probes was mounted near the pipe exit to ensure constant flow conditions between different experiments. Three probes were installed in a specially constructed module, also shown in Fig. 1. The probes were mounted at an axial distance of 20 mm and placed on a traversing mechanism that allowed their accurate radial positioning. For the current experiments in vertical slug flow the probes were installed at the pipe centerline. The measurement module was installed between the pipe sections and could be moved easily along the pipe. The locations of the measuring stations for both pipes are given in Table 1.

The output signals were usually digitized continuously for 3600 s at a sampling frequency of 1 kHz per probe. In order to validate that the results were not affected by the sampling frequency, additional experiments were carried out with a sampling frequency of 10 kHz per probe and duration of 600 s.

3. Data processing

The return signals of the optical probes were sampled by an A/D converter and stored in a data file. In order to get rid of noise the raw signal was processed and a TTL-signal free of noise was obtained. An example of two TTL-signals obtained from two adjacent probes is shown in Fig. 2(a). The low value corresponds to water and the high value to air. The distinction between the elongated bubble (EB) and the liquid slug (LS) regions can be clearly seen. The elongated bubble region is characterized by a long gas duration while in the liquid slug region a frequent occurrence of gas/liquid and liquid/gas transitions is observed due to the small bubbles that are dispersed in the liquid slug. The term "transition times", t_{TR}, refers here to the instants of transition from gas to liquid or vice versa relative to an initial reference time. A bubble duration can be determined from two successive transition times, i.e. the time difference between a liquid/gas and a successive gas/liquid transition.

Due to the different timescales of the elongated bubbles and the small dispersed bubbles in the liquid slug region a threshold could be chosen to filter the small bubbles in the liquid slug out of

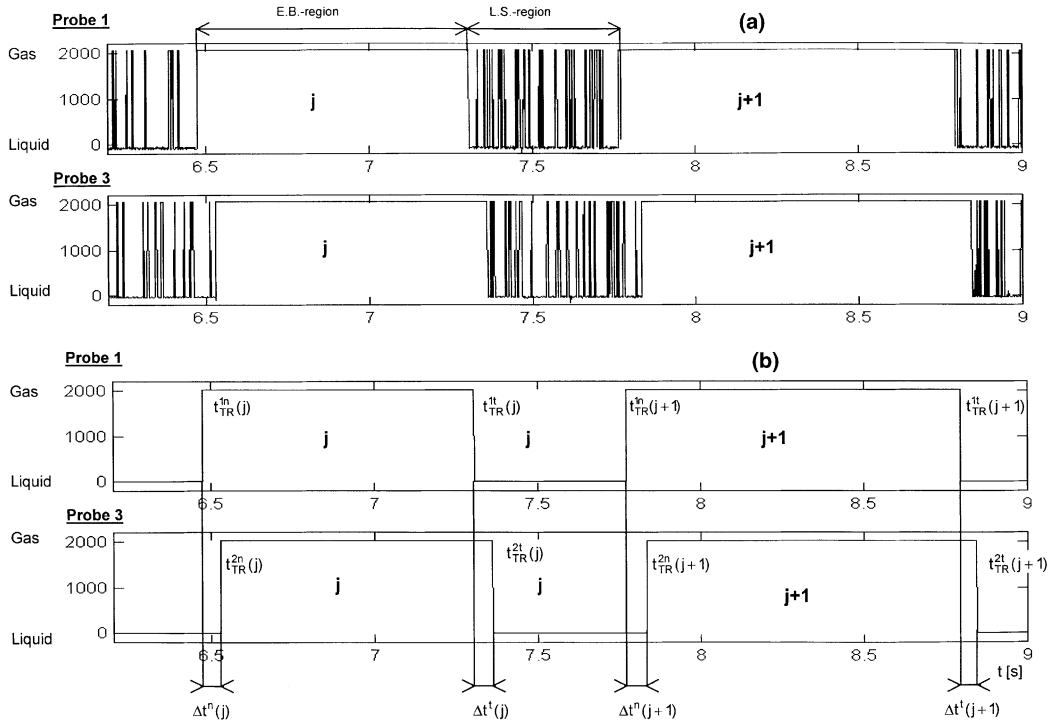

Fig. 2. Signals of two optical probes mounted at an axial distance of 0.04 m: (a) raw sampled signals; (b) filtered (TTL) signals.

the TTL-signal. An example of a filtered TTL-signal is shown in Fig. 2(b) for two probes separated by a small distance. Two elongated bubbles, numbered j and $j+1$, moving from probe 1 to probe 2 are shown. The transition times of nose (n) and tail (t) for the first bubble (j) passing by the first probe (1) are $t_{\mathrm{TR}}^{1\mathrm{n}}(j)$ and $t_{\mathrm{TR}}^{1\mathrm{t}}(j)$, respectively.

The filtering procedure is as follows. The duration (or residence time) of a bubble j passing by probe i is $\Delta t_{\mathrm{B}} = t_{\mathrm{TR}}^{i\mathrm{t}}(j) - t_{\mathrm{TR}}^{i\mathrm{n}}(j)$. The corresponding bubble length is estimated as $\ell_{\mathrm{B}} = U_{\mathrm{tr}} \cdot \Delta t_{\mathrm{B}}$, where U_{tr} is a characteristic translational velocity determined by the application of a cross-correlation technique, as discussed in sequel (Method II). Bubbles longer than a selected threshold for the minimum elongated bubble length, $\ell_{\mathrm{th}} = D$, are considered to be elongated bubbles.

In order to convert the time duration of the elongated bubbles and liquid slugs into actual lengths, the propagation velocities of the interfaces are needed. The experimental approach adopted in the present study made it possible to detect separately the transition times of the nose and the tail of each individual bubble at two successive probes. The knowledge of the time intervals required for a given interface to travel between two probes and the distance between the probes enables the determination of the local instantaneous propagation velocity of nose and tail of each elongated bubble. This information, together with the residence time of each individual Taylor bubble and liquid slug is then applied to obtain their corresponding lengths. The procedure was, however, not as deterministic as it appeared due to the bubble interface distortions. For

vertical flow, both elongated bubble nose and tail exhibit strong oscillations (Polonsky et al., 1999a; Aladjem Talvy et al., 2000). Due to the oscillations the extreme points of the elongated bubble nose and tail do not necessarily coincide with the probe tip installed at the pipe centerline. Fig. 3 shows examples of snapshots of the distorted elongated bubble nose interfaces as recorded by a camera at 7 m from the inlet section for the 0.024 m pipe diameter. The separation distance between the leading and the trailing bubble was quite large, approximately $13D$. It can be clearly seen that the bubble nose sways from one side to the other. This causes some error in the determination of the transition times, leading to errors in the determination of the instantaneous translational velocities. To reduce these errors, advantage was taken of the fact that the distribution of the time intervals required for a given interface (bubble nose or tail) to travel from one probe to the other is approximately normal. The accumulated data on these time intervals for each interface, flow condition and measuring station were plotted on a normal probability plot. An example of such a plot for the instantaneous nose velocities at station E for the 0.024 m pipe diameter is shown in Fig. 4(a). A best fit to the normally distributed data was determined and the outliers (which in this case constitute less than 5% of the total ensemble) of the distribution were discarded. The histogram of the time intervals of Fig. 4(a) is given in Fig. 4(b), together with the fitted Gaussian curve. The characteristic interface propagation velocity at each station and flow condition is determined based on the mean time interval of the best-fitted normal distribution. This method for the determination of the characteristic translational velocity is referred to as Method I in sequel.

A second method (Method II) to determine the characteristic translational velocity is by cross-correlating the TTL-output signals from two probes, mounted a small distance apart. The time lag corresponding to the maximum cross-correlation coefficient determines the most probable time lag, Δt_{cr}, for a gas–liquid interface to move from one probe to the other. The cross-correlation

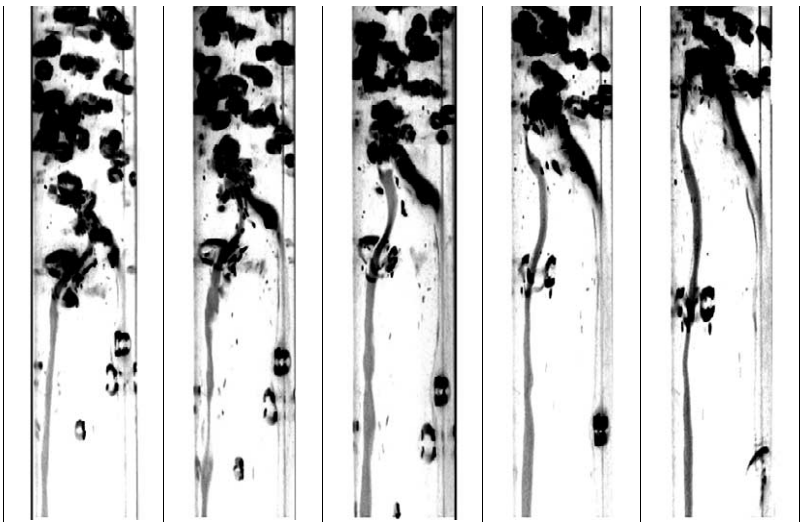

Fig. 3. Series of images of a swaying bubble nose in a continuous slug flow. $D = 0.024$ m, time interval between frames $\Delta t = 0.017$ s.

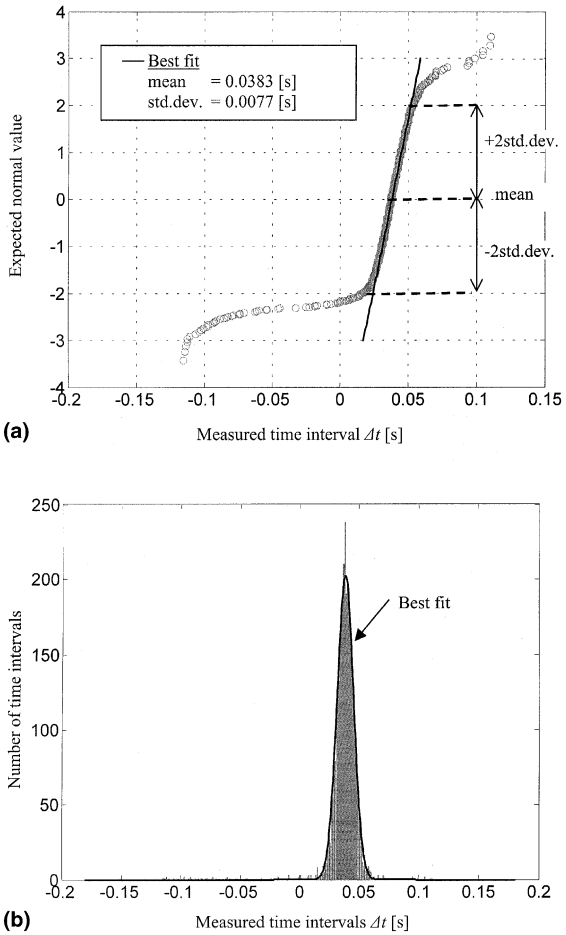

Fig. 4. Distribution of time intervals for the bubble nose: (a) normal probability plot; (b) histogram. $D = 0.024$ m, $U_{LS} = 0.10$ m/s, $U_{GS} = 0.63$ m/s.

procedure could be applied either to the raw TTL signal (Fig. 2(a)) or to the filtered signal (Fig. 2(b)). This procedure does not discriminate between nose and tail. The cross-correlation could be performed between different pairs of probes, i.e. between probes 1 and 2, 1 and 3 or 2 and 3. Examples of the variation of the cross-correlation coefficient with time obtained at various stations are shown in Fig. 5. It can be seen that at station A (near the entrance) the values of the cross-correlation coefficients are lower than those at more remote stations. This is due to the fact that at station A slug flow is still relatively undeveloped. The cross-correlation coefficients of the filtered signal are somewhat higher than those of the raw TTL signals, but the time lags corresponding to the maxima, Δt_{cr}, remain nearly the same.

By using Methods I or II, a characteristic translational velocity is obtained at each station for any given operational condition. The liquid slug and Taylor bubble lengths distributions at each station can be calculated by multiplying the corresponding measured residence time distributions by the appropriate characteristic velocity. A more precise approach for determining the length

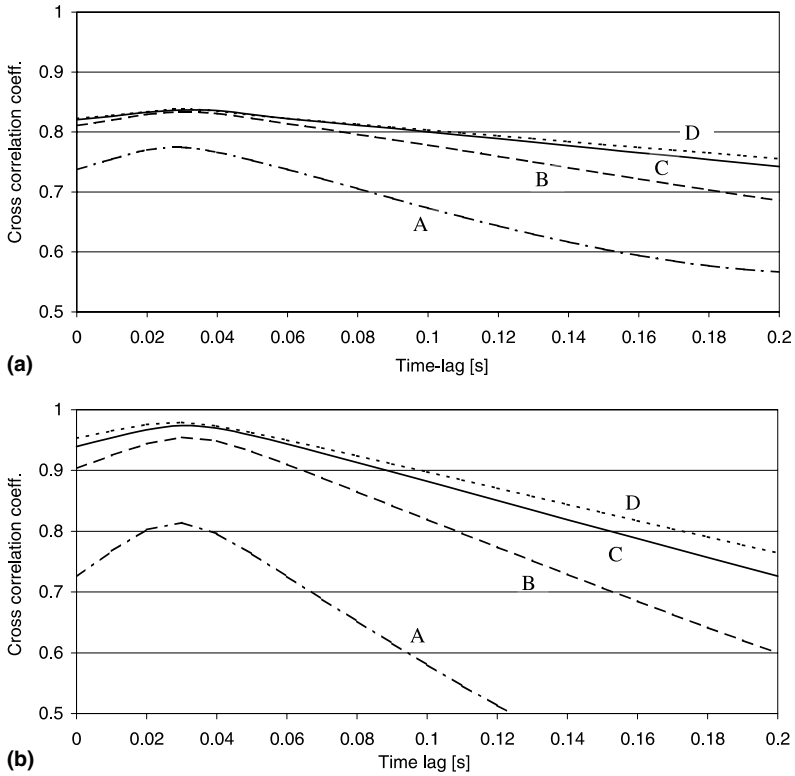

Fig. 5. Cross-correlation coefficient as a function of time lag at various measuring stations: (a) raw signal, (b) filtered TTL signal. $D = 0.054$ m, $U_{LS} = 0.10$ m/s, $U_{GS} = 0.63$ m/s.

distributions is by using the instantaneous propagation velocities of nose and tail of each individual bubble. This approach is described in more detail in Section 4.2.

4. Results

4.1. Evolution of the Taylor bubble characteristic translational velocities along the pipe

The measured translational velocities of the Taylor bubbles as a function of position along the pipe are presented in Figs. 6 and 7 for various flow conditions and both pipe diameters. The results are given separately for the two methods of processing as described in Section 3. To facilitate comparison of data obtained in different experiments, the velocities were normalized by the translational velocities calculated by Nicklin's correlation (Eq. (1) with $C = 1.2$). Since the gas superficial velocity increases along the pipe due to gas expansion, the mixture velocity in (1) at each station along the pipe was adjusted accordingly. In the present experiments, the gas rotameter readings were calibrated according to the conditions prevailing at the pipe exit, i.e. 0.1 MPa. The effective volumetric gas flow rate along the pipe was recalculated taking into

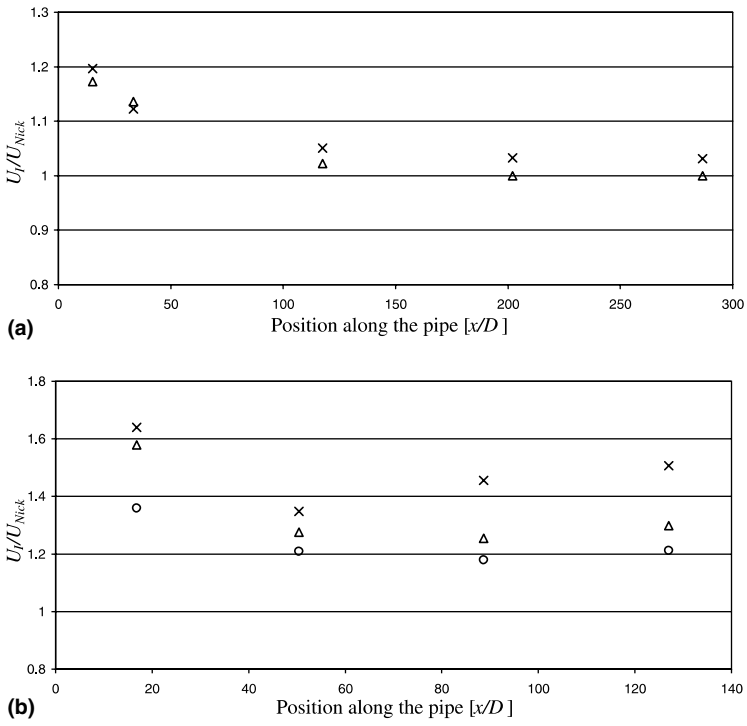

Fig. 6. Variation along the pipe of the Taylor bubble translational velocity (Method I): (×) $U_{LS} = 0.01$ m/s, $U_{GS} = 0.41$ m/s; (△) $U_{LS} = 0.10$ m/s, $U_{GS} = 0.63$ m/s; (◯) $U_{LS} = 0.25$ m/s, $U_{GS} = 0.41$ m/s. (a) $D = 0.024$ m; (b) $D = 0.054$ m.

account the pressure drop along the pipe (Barnea, 1990) and was used to calculate the translational velocity, U_{Nick}, at each station. The results are shown in Table 2 for different stations and various flow rates. As can be seen, Nicklin's translational velocity increases steadily from station to station. Note that the values at the exit of the pipes correspond to the gas superficial velocity as given in Table 2.

The translational velocities were first calculated according to Method I, i.e. using the mean value of the best-fitted Gaussian distribution of the time lags of interface passages between two probes. Computations were performed separately for nose and tail. For all cases the standard deviations of the time interval distributions for the tails were higher (up to 20%) than those for the noses. This is due to the more complex behavior of the Taylor bubble tail (Polonsky et al., 1999a). At each station, the mean measured time lags for tail and nose were nearly the same. The evolution of the nose velocities along the pipe calculated by method I using probes 1 and 3 is presented in Fig. 6(a) ($D = 0.024$ m) and (b) ($D = 0.054$ m).

The characteristic translational velocities calculated using the cross-correlation procedure (Method II) are given in Figs. 7(a) and (b). The cross-correlation was calculated for the filtered TTL-signals (see Fig. 2(b)) obtained by probes 1 and 3. The error in the velocity determination by the application of this method, resulting mainly from the finite sampling frequency, is estimated to be within 4% of the measured interface velocity. The agreement between the velocities obtained by these two independent methods is quite good.

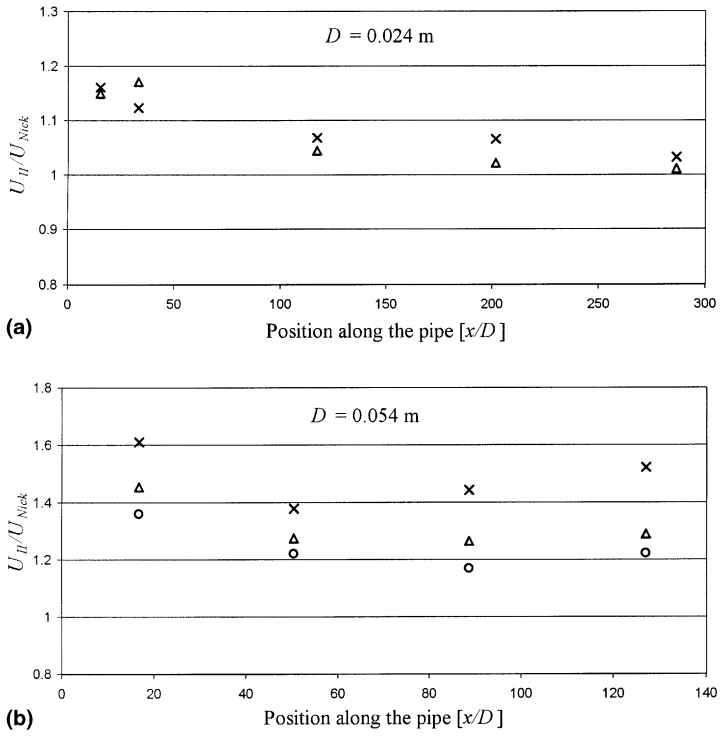

Fig. 7. Variation along the pipe of the Taylor bubble translational velocity (Method II): (×) $U_{LS} = 0.01$ m/s, $U_{GS} = 0.41$ m/s; (△) $U_{LS} = 0.10$ m/s, $U_{GS} = 0.63$ m/s; (◯) $U_{LS} = 0.25$ m/s, $U_{GS} = 0.41$ m/s. (a) $D = 0.024$ m; (b) $D = 0.054$ m.

Table 2
Effect of gas expansion on Nicklin's translational velocity

Flow rate	$D = 0.054$ m			$D = 0.024$ m	
U_{LS} (m/s)	0.01	0.10	0.25	0.01	0.10
U_{GS} (m/s)	0.41	0.63	0.41	0.41	0.63
Station	U_{Nick} (m/s)			U_{Nick} (m/s)	
A	0.64	0.95	0.89	0.56	0.87
B	0.66	0.98	0.91	0.57	0.88
C	0.68	1.02	0.95	0.59	0.91
D	0.71	1.07	0.99	0.61	0.94
E				0.64	0.99
Exit of pipe	0.76	1.13	1.05	0.67	1.04

The shape of the curves in Figs. 6 and 7 is characterized by higher velocities near the inlet of the pipe (station A) and by a decrease in velocities further along the pipe (stations B, C, D and E). For the 0.024 m pipe diameter, Figs. 6(a) and 7(a), the ratio of the measured translational velocity and U_{Nick} approaches unity near the pipe exit, as expected for a developed slug flow. In contrast to

this, for the 0.054 m pipe diameter, Figs. 6(b) and 7(b), this ratio remains notably higher than unity and does not fall below about 1.2 even close to the pipe exit. A possible reason for this is that at the last measurement station the slug flow is still not fully developed.

4.2. Liquid slug and Taylor bubble length distributions

In addition to obtaining the instantaneous local propagation velocity of each individual interface and the residence time of each phase, the adopted experimental technique allows the determination of the propagating velocity of each individual bubble together with the liquid slug length ahead of it. Consider a pair of consecutive bubbles in continuous slug flow, j and $j+1$. The instantaneous translational velocity of the trailing bubble, $j+1$ (see Fig. 2(b)), is defined by its nose movement:

$$U_{\mathrm{tr}}^{n}(j+1) = \frac{\Delta x}{\Delta t^{\mathrm{n}}(j+1)}, \tag{2}$$

where Δx is the distance between the two probes. The liquid slug length between the leading and trailing bubble is given by

$$\ell_{\mathrm{s}}(j) = \langle \Delta t_{\mathrm{s}} \rangle \cdot U_{\mathrm{tr}}^{\mathrm{t}}(j), \tag{3}$$

where $\langle \Delta t_{\mathrm{s}} \rangle$ is defined as the average liquid slug duration measured by both probes

$$\langle \Delta t_{\mathrm{s}} \rangle = \left[\left(t_{\mathrm{TR}}^{1\mathrm{n}}(j+1) - t_{\mathrm{TR}}^{1\mathrm{t}}(j) \right) + \left(t_{\mathrm{TR}}^{2\mathrm{n}}(j+1) - t_{\mathrm{TR}}^{2\mathrm{t}}(j) \right) \right] / 2 \tag{4}$$

and $U_{\mathrm{tr}}^{\mathrm{t}}(j)$ is the measured tail velocity of the leading bubble j which is assumed to remain constant in the process of the liquid slug movement along the probe.

Similarly, the length of each Taylor bubble is determined by

$$\ell_{\mathrm{B}}(j) = \langle \Delta t_{\mathrm{B}} \rangle \cdot U_{\mathrm{tr}}^{\mathrm{n}}(j), \tag{5}$$

where $\langle \Delta t_{\mathrm{B}} \rangle$ is the averaged Taylor bubble duration measured by the two probes and $U_{\mathrm{tr}}^{\mathrm{n}}(j)$ is the measured nose velocity of bubble j.

For each flow condition and measurement station, this procedure enables one to determine the dependence of the translational velocity of each trailing bubble $U_{\mathrm{tr}}^{\mathrm{n}}(j+1)$ on the liquid slug length $\ell_{\mathrm{s}}(j)$ in front of it. The histograms showing the distribution of liquid slug lengths are given in Figs. 8 and 9. The bin size in these histograms is the pipe diameter D. For each bin separately, the corresponding trailing bubble velocities were averaged. The outliers in the time lag distributions (cf. Fig. 4) were discarded similarly to the procedure applied in Method I. This filtering effectively resulted in a considerable reduction of the ensemble size over which the averaging in each bin has been carried out.

Figs. 8 and 9 present the evolution of liquid slug length distributions along the pipe, together with the corresponding instantaneous trailing bubble velocity for the two pipe diameters and various flow conditions. The trailing bubble velocity is shown as a function of liquid slug length ahead of it. The trailing bubble velocity (secondary y-axis) is normalized in each frame by the local Nicklin's translational velocity. The histograms (primary y-axis) show the percentage of the total number of liquid slugs that are used for calculating the average of the instantaneous

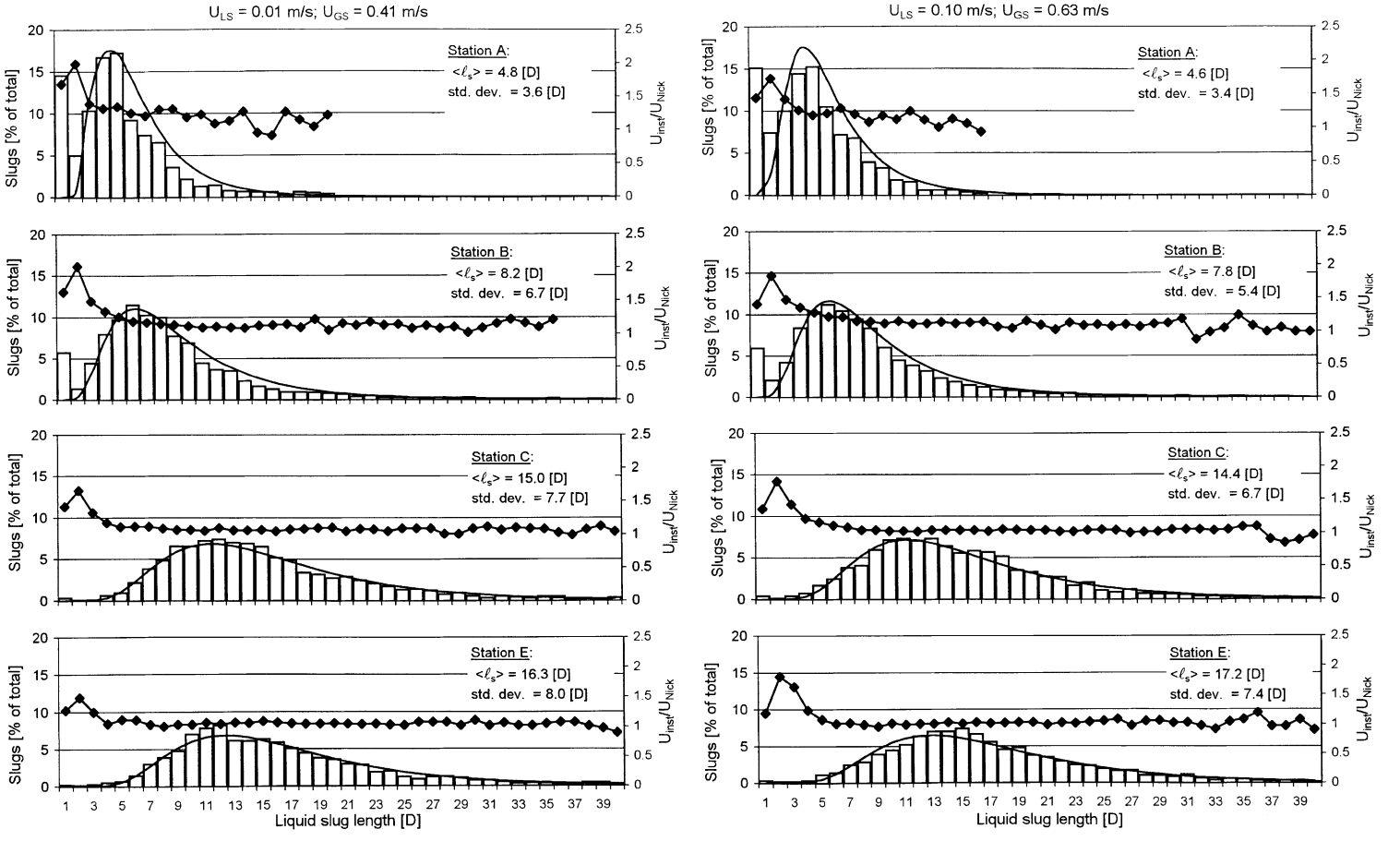

Fig. 8. Instantaneous translational velocity as a function of separation distance, and the liquid slug length distribution based on the instantaneous velocity, at various positions along the pipe, $D = 0.024$ m. (–◆–) $U_{\text{inst}}/U_{\text{Nick}}$, (—) log-normal fit.

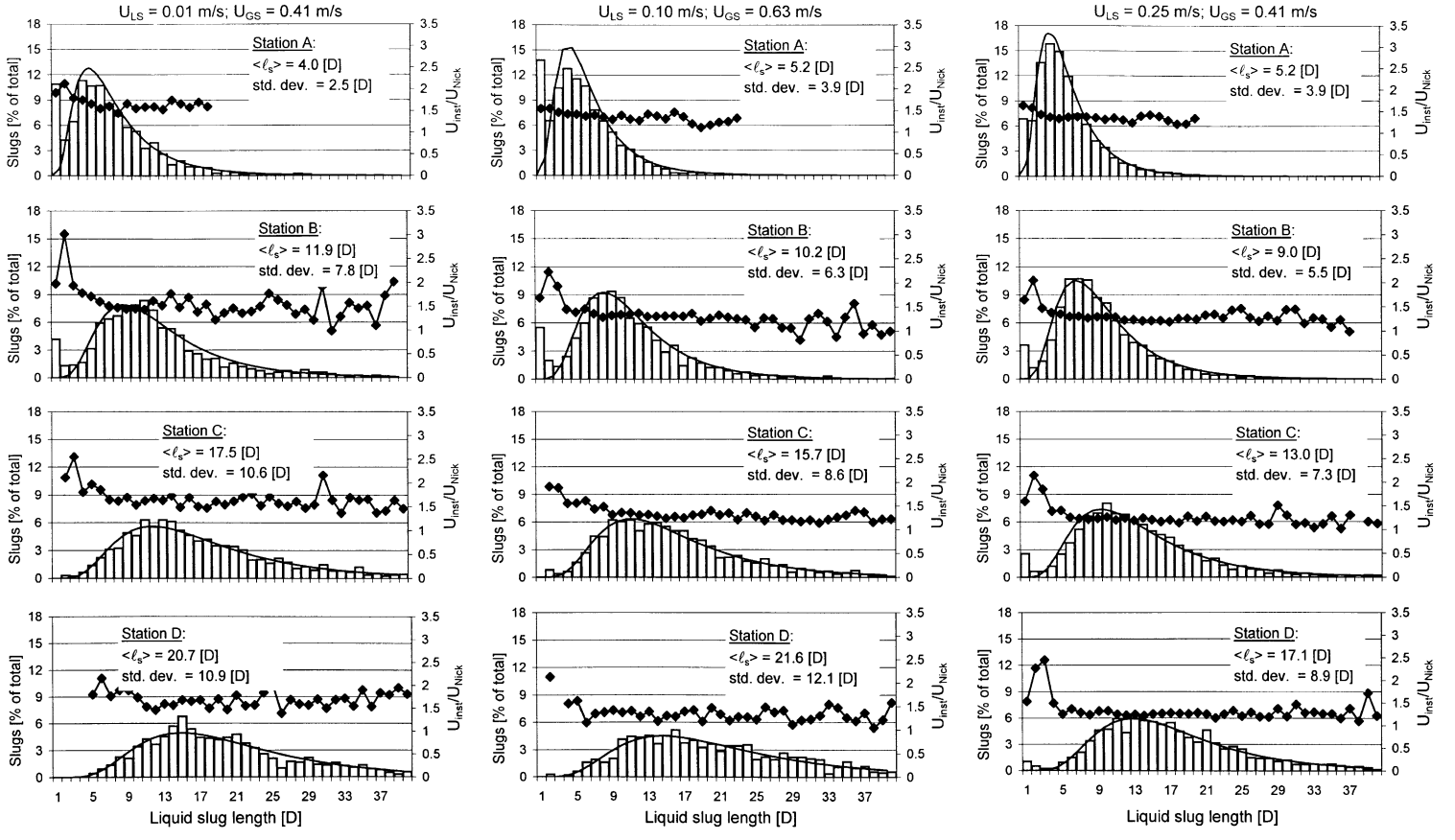

Fig. 9. Instantaneous translational velocity as a function of separation distance, and the liquid slug length distribution based on the instantaneous velocity, at various positions along the pipe, $D = 0.054$ m. (–◆–) $U_{\text{inst}}/U_{\text{Nick}}$, (—) log-normal fit.

Table 3
Parameters ξ and σ of the log-normal fit (Eq. (6))

U_{LS} (m/s)	0.01					0.10					0.25				
U_{GS} (m/s)	0.41					0.63					0.41				
Station	A	B	C	D	E	A	B	C	D	E	A	B	C	D	E
$D = 0.054$ m: *liquid slugs*															
ξ	1.80	2.38	2.71	2.90		1.61	2.27	2.62	2.93		1.54	2.09	2.46	2.74	
σ	0.62	0.53	0.54	0.49		0.60	0.50	0.52	0.54		0.578	0.53	0.53	0.48	
$D = 0.024$ m: *liquid slugs*															
ξ	1.54	1.98	2.58		2.63	1.52	1.94	2.55		2.68					
σ	0.55	0.59	0.49		0.46	0.57	0.57	0.48		0.46					
$D = 0.054$ m: *Taylor bubbles*															
ξ	1.27	2.00	2.55	2.72		1.12	2.14	2.62	2.82		0.69	1.36	1.70	1.94	
σ	0.56	0.59	0.48	0.46		0.64	0.43	0.47	0.47		0.44	0.42	0.41	0.39	
$D = 0.024$ m: *Taylor bubbles*															
ξ	1.69	2.59	3.10		3.35	1.74	2.53	3.18		3.47					
σ	0.56	0.48	0.37		0.34	0.64	0.54	0.41		0.35					

velocities measured for each value of the leading slug length. Note that the ensemble size at each station exceeded 10^3.

It can be clearly seen that the distributions of the liquid slug lengths are visibly skewed. A best fit to the log-normal distribution was therefore attempted, and the resulting distribution curve is also plotted in these figures. The probability density function of the log-normal distribution (see, e.g. Miller and Freund, 1965) is

$$f(x) = \frac{1}{\sqrt{2\pi}\sigma}\left(\frac{\ell_s}{D}\right)^{-1} \exp -1/2\left[\frac{\ln(\ell_s/D) - \xi}{\sigma}\right]^2 \tag{6}$$

with $x > 0$, and $\sigma > 0$. The parameters ξ and σ are given in Table 3 for all cases.

Near the entrance (station A), the distributions are peaked around relatively small values of few pipe diameters. Further along the pipe the distributions become less peaked with an increase in the most probable and mean values of slug lengths.

The curves in Figs. 8 and 9 showing the dependence of the instantaneous velocities of the Taylor bubbles on the liquid slug length ahead of them, $U_{tr} = f(\ell_s)$, exhibit a typical behavior for all cases. For separation distances smaller than $3D$ there is a significant acceleration of Taylor bubbles. The maximum normalized trailing bubble velocities lie between 1.5 and 3, which compares favorably with the maximum values determined by Aladjem Talvy et al. (2000). However, for very short separation distances (up to $1D$), the instantaneous velocity abruptly decreases. This phenomenon can be explained by the fact that prior to coalescence there exists a small liquid "bridge" between leading and trailing bubbles and the trailing bubble travels approximately with the velocity of the leading one, as visualized by Aladjem Talvy et al. (2000) in experiments with controlled bubble injection. At larger separation distances, the Taylor bubble velocities decrease gradually. At very large separation distances, considerable scatter in the velocity data is obtained due to insufficient ensemble size at these conditions. The Taylor bubble propagation velocity in

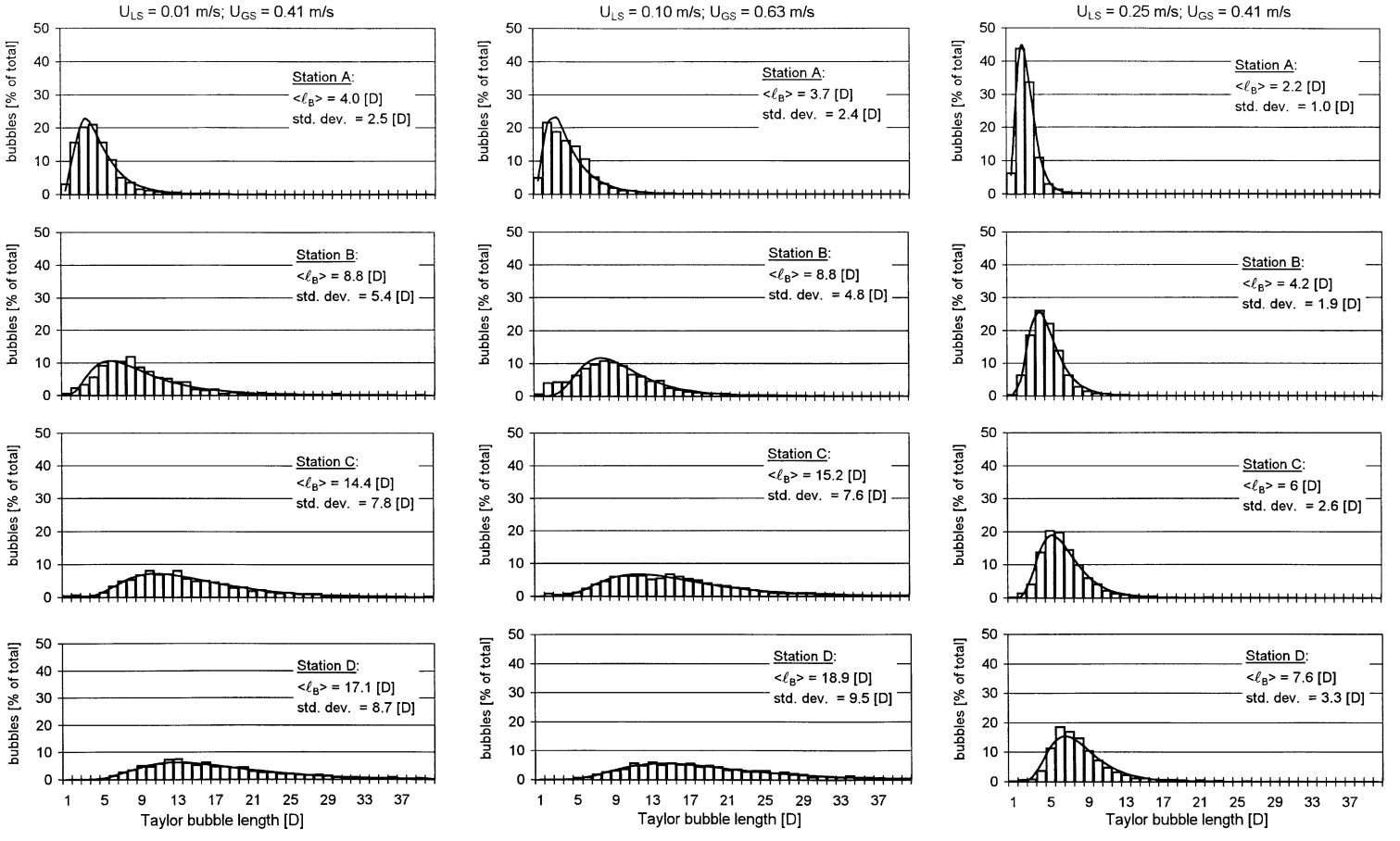

Fig. 10. Taylor bubble length distribution based on the instantaneous velocity, at various positions along the pipe, $D = 0.054$ m. (—) Log-normal fit.

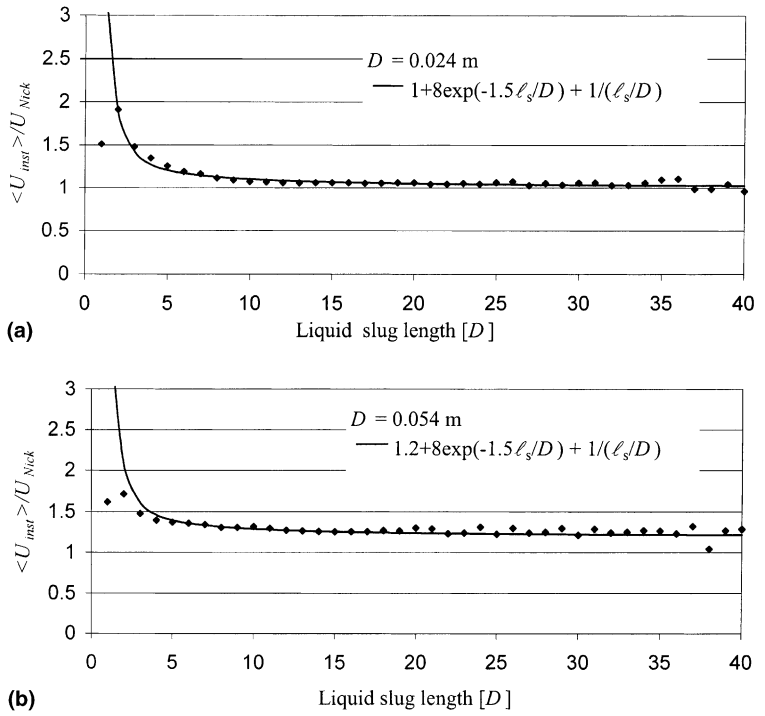

Fig. 11. Averaged translational velocity of Taylor bubbles as a function of the liquid slug length ahead of them: (a) $D = 0.024$ m; (b) $D = 0.054$ m.

the 0.024 m diameter pipe approaches the corresponding Nicklin's velocities at large separation distances (Fig. 8), while in the 0.054 m diameter pipe the Taylor bubble velocities remain considerably higher than those predicted by Nicklin's correlation with $C = 1.2$ (Fig. 9).

Fig. 10 depicts the distributions of the Taylor bubble lengths in the 0.054 m diameter pipe. As it was observed for the liquid slugs, the distributions are skewed and the best-fitted log-normal curve is plotted for each flow condition and at each measuring station. The coalescence process along the pipe results in a gradual increase of the most probable and the mean values of the Taylor bubble length. Accordingly, the distributions at increasing distances from the pipe inlet become more flat.

The accumulated information on the dependence of the Taylor bubble velocities on the liquid slug length ahead of them for different flow conditions and measuring stations is averaged, for each pipe diameter separately. The weighted average of the normalized velocities for each separation distance is presented in Fig. 11(a) for $D = 0.024$ m and in Fig. 11(b) for $D = 0.054$ m. The best-fit curve suggested by Moissis and Griffith (1962) is adopted here with some modifications:

$$\frac{U_{\mathrm{tr}}}{U_{\mathrm{Nick}}} = a + b\exp(-c\ell_{\mathrm{s}}/D) + \frac{1}{\ell_{\mathrm{s}}/D}. \tag{7}$$

The translational velocities of the elongated bubble for both pipes are normalized by Nicklin's correlation (1) with $C = 1.2$. The coefficient a in (7) represents the normalized terminal elongated bubble propagation velocity for large separation distances. For the case of $D = 0.024$ m, $a = 1.0$,

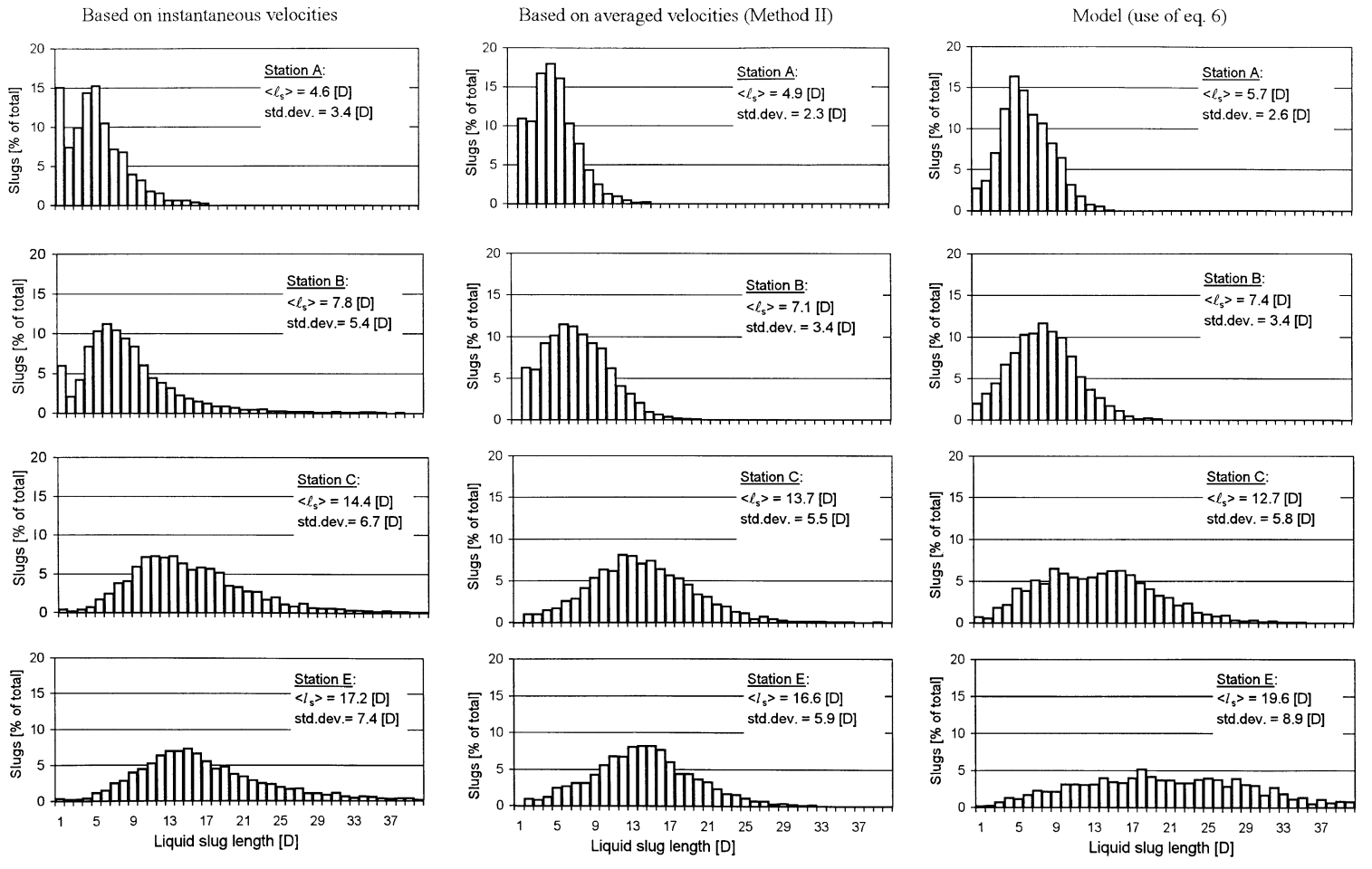

Fig. 12. Comparison between measured and computed liquid slug length distributions for different positions along the pipe: $D = 0.024$ m; $U_{LS} = 0.10$ m/s; $U_{GS} = 0.63$ m/s.

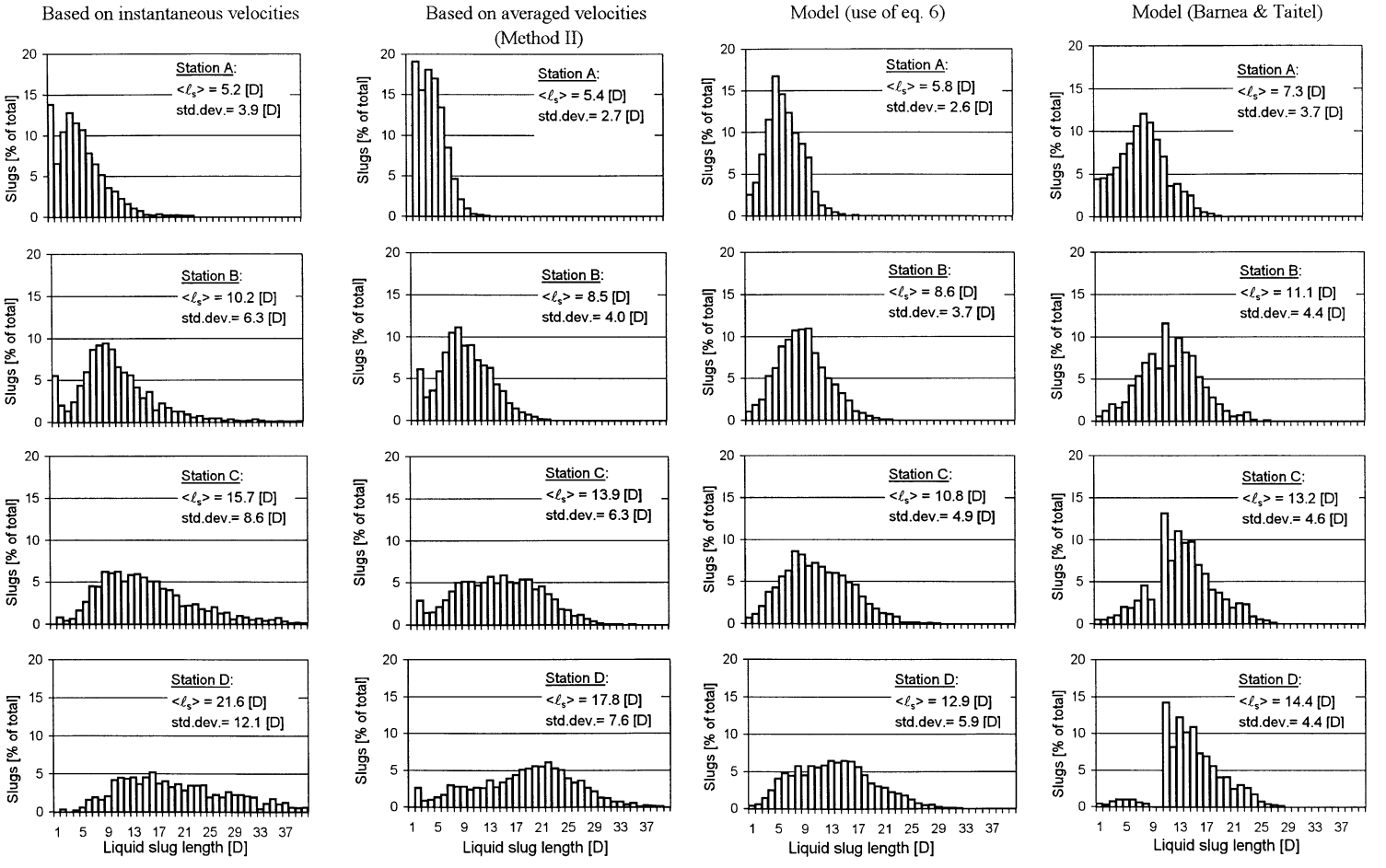

Fig. 13. Comparison between measured and computed liquid slug length distributions for different positions along the pipe: $D = 0.054$ m; $U_{LS} = 0.10$ m/s; $U_{GS} = 0.63$ m/s.

while for $D = 0.054$ m a notable higher value of $a = 1.2$ is obtained. The last term, which is absent in the Moissis and Griffith correlation, is added to account for the slower decay in the translational velocity of elongated bubbles behind relatively long slugs. The decrease in the trailing bubble velocity observed for very short separation distances due to the bridging effect is disregarded in (7) since in these cases the bubble merging is imminent. For both pipe diameters, the coefficient $b = 8.0$ is in agreement with Moissis and Griffith. The coefficient c in both cases has the value of 1.5. The resulting equation (7) for $D = 0.024$ m also fits the data obtained in a different facility by Aladjem Talvy et al. (2000). It should be stressed that in the current study, the relation (7) between the trailing bubble velocity and the liquid slug length ahead of it is obtained for naturally occurring continuous slug flow. Similar correlations available in the literature were obtained for controlled injection of individual bubbles.

The relation between the trailing elongated bubble and the slug length ahead of it is required as input to a model describing the evolution of slug length distribution along the pipe (Barnea and Taitel, 1993). The model tracks each bubble as it propagates down the pipe. The positions of nose and tail of the Taylor bubbles at each time step are determined according to the instantaneous translational velocities of nose X_j and tail Y_j:

$$X_j(t + \Delta t) = X_j(t) + U_j^{\mathrm{n}}(t)\Delta t, \tag{8}$$

$$Y_j(t + \Delta t) = Y_j(t) + U_j^{\mathrm{t}}(t)\Delta t, \tag{9}$$

where $U_j^{\mathrm{n}} = f(Y_{j-1} - X_j) = f(\ell_{\mathrm{s}})$, ℓ_{s} is the liquid slug length ahead of the trailing bubble, and $U_j^{\mathrm{n}} = U_j^{\mathrm{t}}$. In the present study, correlation (7) with the coefficients appropriate for each pipe diameter was used to define the function $f(\ell_{\mathrm{s}})$. The model was applied assuming a random uniform length distribution of the liquid slug lengths at the entrance to the pipe within the range $2D \leqslant \ell_{\mathrm{s}} \leqslant 6D$. It has been shown (Barnea and Taitel, 1993) that the evolution of the lengths distribution along the pipe is not sensitive to the shape of the initial distribution. The model results are obtained at the locations corresponding to the measuring stations in the experiments.

The model predictions for the evolution of slug length distribution along the pipe are compared with the experimental results. Such a comparison for $D = 0.024$ m is presented in Fig. 12 and for $D = 0.054$ m in Fig. 13. The superficial gas and liquid velocities in these examples are: $U_{\mathrm{LS}} = 0.10$ m/s, $U_{\mathrm{GS}} = 0.63$ m/s.

The first column in Figs. 12 and 13 presents the slug length distributions based on the directly measured instantaneous velocity of each interface. An alternative simplified procedure to obtain the slug length distributions from the experimental data is to multiply the measured distributions of the time duration of the liquid slugs at each station by the local constant characteristic translational velocity, as determined by the application of Methods I or II (see Section 3). The results obtained by using the characteristic velocities based on the cross-correlation procedure (Method II) are shown in the second column of Figs. 12 and 13. The third column shows the corresponding results obtained by application of the Barnea and Taitel (1993) model using correlation (7).

The simplified procedure (column 2) yields distributions similar to those of the exact approach (column 1). However, the skewness of the distributions obtained by the simplified procedure is less pronounced. In general, the shape and the development of the distributions along the pipe in the experiments and in the model calculations are quite similar. Although the slug length distribution

at the pipe entrance is arbitrary in the model computations, the resulting distributions evolving along the pipe are quite similar to the experimental data, both in their shapes and in the mean values. In Fig. 13 an additional column is added in which the results of computations are shown using the correlation employed by Barnea and Taitel (1993). In this correlation, a concept of a minimum stable slug length $\ell_{\min}$ is adopted. The model results in this case show that slugs shorter than $\ell_{\min}$ are effectively eliminated far from the pipe inlet. This is in a clear disagreement with the experiments.

Fig. 14 demonstrates the variation of the sampled ensemble size N (the total number slug units sampled) along both pipes. The values of N are normalized by the corresponding ensemble size at the pipe exit, N_{exit}. The values of N_{exit} are also given in this figure. The variation of the ensemble size along the pipe represents the coalescence rate. This rate appears to be essentially independent of the pipe diameter and flow conditions. The coalescence rate essentially defines the extent of the entrance length of slug flow. This rate remains quite high up to approximately $x/D = 60$ in both pipes. A steady state is not achieved even at the last two measuring stations in both pipes.

The evolution of the mean values of the length distributions is presented in Fig. 15 for all flow rates studied here. A comparison between the measured and the computed mean liquid slug lengths at various stations along the pipe is shown in Fig. 15(a) for $D = 0.024$ m and in Fig. 15(b) for $D = 0.054$ m. The corresponding information regarding the mean Taylor bubble lengths is shown in Figs 15(c) and (d). In general, the mean length increases along the pipe, with rates of growth becoming more moderate toward the pipe exit. The coalescence of consecutive Taylor bubbles in an undeveloped slug flow causes an increase in both the liquid slug and Taylor bubble lengths. Moreover, gas expansion due to pressure drop contributes to an additional increase in the Taylor bubble lengths. A very good agreement is obtained between the model predictions and the experimental results for both liquid slugs and Taylor bubbles lengths in the 0.024 m pipe diameter (Figs. 15(a) and (c)). In the larger pipe ($D = 0.054$ m) the agreement is quite good in the first half of the pipe, while farther from the entrance the model underpredicts the lengths of both slugs and Taylor bubbles.

It can be seen from Fig. 15 that at each station the mean measured dimensionless liquid slug lengths seem to be almost insensitive to the flow rates and to the pipe diameter. Contrary to this, the mean measured Taylor bubble lengths depend on the flow rate and on the pipe diameter. The values of the Taylor bubble lengths are considerably higher for $D = 0.024$ m than those for

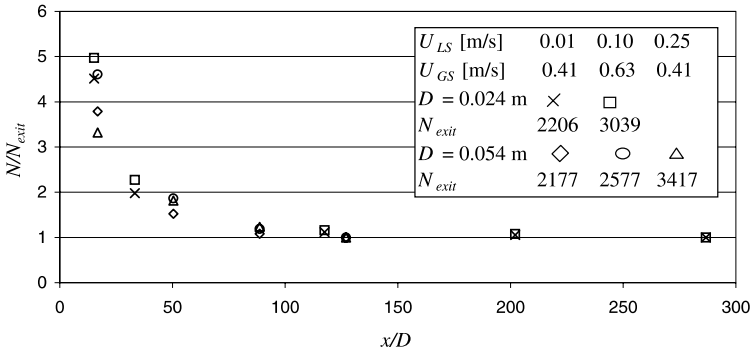

Fig. 14. Variation of the ensemble size along the pipe.

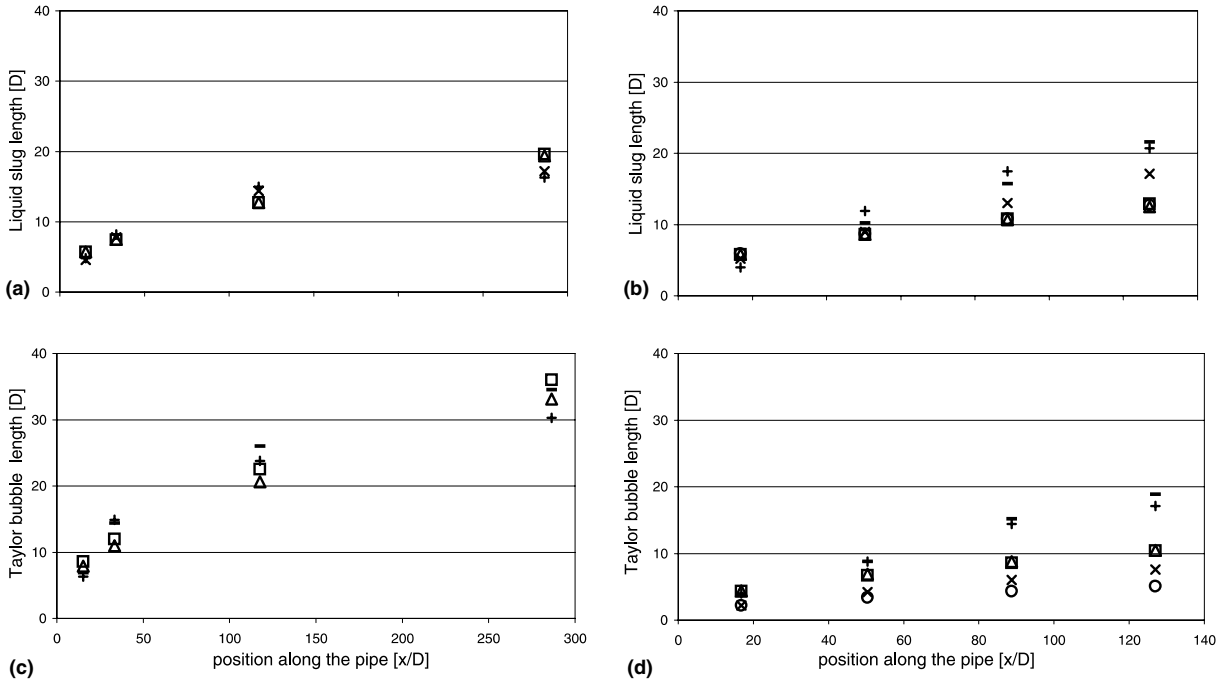

Fig. 15. Mean liquid slug and Taylor bubble lengths as a function of the position along the pipe. Model: ($\triangle$) $U_{LS} = 0.01$ m/s, $U_{GS} = 0.41$ m/s; ($\square$) $U_{LS} = 0.10$ m/s, $U_{GS} = 0.63$ m/s; ($\bigcirc$) $U_{LS} = 0.25$ m/s, $U_{GS} = 0.41$ m/s. Exp: ($+$) $U_{LS} = 0.01$ m/s, $U_{GS} = 0.41$ m/s; ($-$) $U_{LS} = 0.10$ m/s, $U_{GS} = 0.63$ m/s; ($\times$) $U_{LS} = 0.25$ m/s, $U_{GS} = 0.41$ m/s. (a) Liquid slug, $D = 0.024$ m; (b) liquid slug, $D = 0.054$ m; (c) Taylor bubble, $D = 0.024$ m; (d) Taylor bubble, $D = 0.054$ m.

$D = 0.054$ m at the same flow rates and at the same dimensionless distance from the pipe entrance. These results can be understood considering the following. The dimensionless liquid slug length depends on the evolution of the liquid flow in the wake of the elongated bubble, which is only weakly sensitive to the pipe diameter and flow rates. For a given liquid slug length ℓ_s, the Taylor bubble length ℓ_B is prescribed by the overall mass balance, which in turn determines the average void fraction in the pipe. Discarding dispersed bubbles in the liquid slug, the average void fraction can be approximated as $\alpha = U_{GS}/U_{tr} \approx \ell_B/(\ell_B + \ell_s)$. For identical dimensionless liquid slug lengths and superficial velocities, U_{tr} is smaller for the pipe of smaller diameter, resulting in a higher dimensionless Taylor bubble length. Similar considerations explain the effect of the flow rate on the Taylor bubble length.

5. Summary and conclusions

A comprehensive study of the evolution of slug flow parameters along the pipe was carried out in vertical flow for two pipe diameters and various flow rates. The instantaneous local void fraction was measured using fiber optic probes at a number of measuring stations along the pipes.

At each station, the gas–liquid interface passage was detected by a set of three adjacent probes. The information provided by the sensors was sampled over a long period of time, recorded by the computer and processed to extract the required statistical and hydrodynamic parameters of the flow.

The variation of the characteristic translational velocity of elongated bubbles along the pipe was obtained by application of two different data processing methods. Both methods yield similar results and indicate that the mean velocity of elongated bubbles decreases along the pipe. For pipe diameter $D = 0.024$ m, the Taylor bubble translational velocity approaches the value suggested by Nicklin et al. (1962), Eq. (1) with $C = 1.2$. In the larger pipe ($D = 0.054$ m), the Taylor bubble translational velocity remains notably higher than that given by Nicklin's prediction even close to the pipe exit.

The simultaneous measurements of the local instantaneous interface velocities and the duration of each phase at the given location made it possible to determine the evolution of liquid slug length and Taylor bubble length distributions along the pipe. The length distributions exhibit considerable skewness at all measuring stations. A log-normal fit is suggested for these distributions. The parameters of the suggested fit are presented. It was observed that short slugs do not disappear even far from the pipe entrance, which indicates that some coalescence persists at these locations. A similar conclusion can be drawn from the measured variation of the ensemble size along the pipe. The information on the maximum liquid slug length at each station can be obtained from the presented distributions. The characteristic values of the maximum slug length at the last station attain the value of about $40D$ in both pipes.

The dependence of the trailing bubble velocity on the liquid slug length ahead of it was determined for all measuring locations. The accumulated body of the experimental data was used to suggest empirical correlations relating the Taylor bubble velocities to the separation distances between the consecutive bubbles in continuous slug flow.

These empirical correlations were employed as an input to a predictive model for computing liquid slug and Taylor bubble length distributions. The computed results compare favorably with the experimental data for the smaller pipe diameter. For the larger pipe diameter, the model results somewhat underpredict the experimental data.

It should be noted that scatter of the results in the larger diameter pipe is much more pronounced. This is due to the fact that the slug flow in this pipe is considerably more complicated. The dimensionless length of the 10 m pipe is notably shorter for $D = 0.054$ m ($185D$) than for $D = 0.024$ m ($420D$). As a result of this, the flow in the larger pipe is less developed. The distortions in the elongated bubble shape are much stronger in this case. This can be attributed in part to weaker effect of the surface tension in larger pipes. In addition, the liquid slug is much more aerated for $D = 0.054$ m. All this results in additional difficulties in the computer processing of the sampled results.

Acknowledgements

This work was partially supported by grants from Israel Science Foundation and Tulsa University Fluid Flow Projects (TUFFP). The authors gratefully acknowledge this support.

References

Aladjem Talvy, C., Shemer, L., Barnea, D., 2000. On the interaction between two consecutive elongated bubbles in a vertical pipe. Int. J. Multiphase Flow 26, 1905–1923.

Barnea, D., Brauner, N., 1985. Holdup of the liquid slug in two phase intermittent flow. Int. J. Multiphase Flow 11, 43–49.

Barnea, D., Taitel, Y., 1993. A model for slug length distribution in gas–liquid slug flow. Int. J. Multiphase Flow 19, 829–838.

Bendiksen, K.H., 1984. An experimental investigation of the motion of long bubbles in inclined tubes. Int. J. Multiphase Flow 10, 467–483.

Bernicot, M., Drouffe, J.M., 1989. Slug length distribution in two-phase transportation systems, In: Proceedings of the Fourth International Conference on Multi-Phase Flow, Nice, France. BHRA, Cranfield, Beds, pp. 485–493.

Brill, J.P., Schmidt, Z., Coberly, W.A., Herring, J.D., Moore, D.W., 1981. Analysis of two-phase tests in large-diameter flow lines in Prudhoe Bay field. Soc. Petr. Eng. J. 271, 363–378.

Cook, M., Behnia, M., 2000. Slug length prediction in near horizontal gas–liquid intermittent flow. Chem. Eng. Sci. 55, 2009–2018.

Costigan, G., Whalley, P.B., 1997. Slug flow regime identification from dynamic void fraction measurements in vertical air–water flows. Int. J. Multiphase Flow 23, 263–282.

Dhulesia, H., Bernicot, M., Deheuvels, P., 1991. Statistical analysis and modelling of slug lengths. In: Proceedings of the Fifth International Conference on Multiphase Production, Cannes, France. BHRA, Cranfield, Beds, pp. 80–112.

Dukler, A.E., Hubbard, M.G., 1975. A model for gas–liquid slug flow in horizontal and near horizontal tubes. Ind. Eng. Chem. Fundam. 14, 337–347.

Fagundes Netto, J.R., Fabre, J., Grenier, P., Péresson, L., 1998. An experimental study of an isolated long bubble in an horizontal liquid flow. In: Proceedings of the Third International Conference on Multiphase Flow, ICMF'98, Lyon, France.

Fernandes, R.C., Semiat, R., Dukler, A.E., 1983. Hydrodynamic model for gas–liquid slug flow in vertical tubes. AIChE J. 29, 981–989.

Hasanein, H.A., Tudose, G.T., Wong, S., Malik, M., Esaki, S., Kawaji, M., 1996. Slug flow experiments and computer simulation of slug length distribution in vertical pipes. In: Proceedings of the AIChE Symposium Series on Heat Transfer, Houston, pp. 211–219.

van Hout, R., Shemer, L., Barnea, D., 1992. Spatial distribution of void fraction within a liquid slug and some other related Slug Parameters. Int. J. Multiphase Flow 18, 831–845.

Miller, I., Freund, J.E., 1965. Probability and Statistics for Engineers. Prentice-Hall, Englewood Cliffs, NJ.

Moissis, R., Griffith, P., 1962. Entrance effects in a two-phase slug low. J. Heat Transfer 84, 366–370.

Nicklin, D.J., Wilkes, J.O., Davidson, J.F., 1962. Two-phase flow in vertical tubes. Trans. Inst. Chem. Eng. 40, 61–68.

Pinto, A.M.F.R., Coelho Pinheiro, M.N., Campos, J.B.L.M., 1998. Coalescence of two gas slugs rising in a co-current flowing liquid in vertical tubes. Chem. Eng. Sci. 53, 2973–2983.

Polonsky, S., Barnea, D., Shemer, L., 1999a. Averaged and time-dependent characteristics of the motion of an elongated bubble in a vertical pipe. Int. J. Multiphase Flow 25, 795–812.

Polonsky, S., Shemer, L., Barnea, D., 1999b. The relation between the Taylor bubble motion and the velocity field ahead of it. Int. J. Multiphase Flow 25, 957–975.

Sæther, G., Bendiksen, K., Müller, J., Frøland, E., 1990. The fractal statistics of liquid slug lengths. Int. J. Multiphase Flow 16, 1117–1126.

Shemer, L., Barnea, D., 1987. Visualization of the instantaneous velocity profiles in gas–liquid slug flow. Phys. Chem. Hydrodyn. 8, 243–253.

Taitel, Y., Barnea, D., Dukler, A.E., 1980. Modelling flow pattern transitions for steady upward gas–liquid flow in vertical tubes. AIChE J. 26, 345–354.

Taitel, Y., Barnea, D., 1990. Two-phase slug flow. Adv. Heat Transfer 20, 83–132.